A Catalytic Cycle Related to Molybdenum Enzymes Containing $[Mo^{VI}O_2]^{2+}$ Oxidized Active Sites

Zhiguang Xiao,*,† Michael A. Bruck,‡ John H. Enemark,‡ Charles G. Young,† and Anthony G. Wedd*,†

School of Chemistry, University of Melbourne, Parkville, Victoria 3052, Australia, and Department of Chemistry, University of Arizona, Tucson, Arizona 85721

Received August 29, 1996[⊗]

Interconversion of mononuclear *cis*-dioxo−Mo(VI) and oxo−Mo(V,IV) complexes of the hydrotris(3,5-dimethylpyrazol-1-yl)borate ligand (L) by one-electron and two-electron reactions is described. In the coordinating solvent pyridine (py), $LMo^{VI}O_2(SPh)$ is reduced by cobaltocene in one-electron steps to stable $LMo^{IV}O(SPh)$-(py). The compound $LMo^{IV}O(SPh)(py)\cdot 0.6MeOH$ crystallizes in orthorhombic space group *Pbca*, with a = 13.790(2) Å, b = 15.266(2) Å, c = 27.807(5), V = 5853(3) Å^3, and Z = 8. The complex exhibits a distorted octahedral structure with a facially tridentate ligand L and mutually *cis* oxo [Mo═O = 1.667(5) Å], pyridine [Mo−N = 2.184(5) Å], and thiolate [Mo−S = 2.390(3) Å] ligands. This and other $LMo^{IV}O(SR)(py)$ (R = Ph, CH_2Ph, $CHMe_2$) complexes are also obtained from $LMo^{VI}O_2(SR)$ via two-electron oxygen atom transfer reactions involving tertiary phosphines in pyridine. In dry solvents, the oxo−Mo(IV) complexes are oxidized by ferrocenium ion to the EPR-active cations $[LMo^{V}O(SR)(py)]^+$ which are hydrolyzed rapidly in wet solvents to $LMo^{V}O(OH)$-(SR). More generally, the complexes $LMo^{VI}O_2X$ (X = Cl, Br, NCS, OPh, SPh, SCH_2Ph, $SCHMe_2$) react with PPh_3 at room temperature to yield $OPPh_3$ and unstable, coordinatively-unsaturated intermediates $LMo^{IV}OX$. The latter are oxidized back to $LMo^{VI}O_2X$ by Me_2SO or can be trapped in a number of ways, depending on available ligands. For example, the complexes $LMo^{IV}OX$(solvent) are detected in coordinating solvents, $LMo^{V}OClX$ in chlorinated solvents, $LMo^{V}O(OMe)X$ in MeOH, and $[LMo^{V}O]_2(\mu$-O) in dry toluene. However, in wet weakly-coordinating solvents, $LMo^{V}O(OH)X$ complexes are produced cleanly and can be oxidized quantitatively to $LMo^{VI}O_2X$. Consequently, $LMo^{VI}O_2X$ complexes are catalysts for the oxidation of PPh_3 by O_2 in the presence of H_2O. Oxygen isotope tracing shows that H_2O rather than O_2 is the source of the oxygen atom which is transferred to PPh_3. This is the first model system which displays the full cycle proposed for oxidizing molybdoenzymes featuring $[Mo^{VI}O_2]^{2+}$ resting states.

Introduction

Molybdenum pterin enzymes catalyze a variety of two-electron-redox reactions involving a net exchange of an oxygen atom between substrate Y and water:[1−5]

$$Y + H_2O = YO + 2H^+ + 2e^- \qquad (1)$$

The majority of these systems can be classified into three families,[3] and recent crystal structures have illuminated the structural base of the xanthine oxidase and dimethyl sulfoxide reductase families.[4] X-ray absorption spectroscopy indicates that the sulfite oxidase family features $[Mo^{VI}O_2]^{2+}$ oxidized active sites.[3,6,7]

Scheme 1

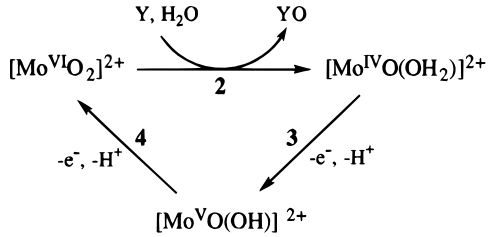

A consensus cycle has evolved for the latter family combining an oxygen atom transfer with two successive one-electron steps that are coupled to proton transfers (Scheme 1).[2] In the oxidation step (reaction 2, Scheme 1), formal two-electron oxygen atom transfer (OAT) from the $[Mo^{VI}O_2]^{2+}$ center to the substrate is followed by aquation to form a $[Mo^{IV}O(OH_2)]^{2+}$ center. The subsequent steps (reactions 3 and 4, Scheme 1) involve the reoxidation of the $[Mo^{IV}O(OH_2)]^{2+}$ center by successive coupled electron−proton transfer (CEPT) reactions. Reductase enzymes would follow Scheme 1 in a counterclockwise direction.

Water is the source of the oxygen atom that is incorporated into substrate in Scheme 1. This role has been confirmed for xanthine oxidase from cow's milk by oxygen isotopic labeling

† University of Melbourne.
‡ University of Arizona.
⊗ Abstract published in *Advance ACS Abstracts,* November 15, 1996.

(1) (a) *Molybdenum Enzymes, Cofactors and Model Systems;* Stiefel, E. I., Coucouvanis, D., Newton, W. E., Eds.; ACS Symposium Series 535; American Chemical Society: Washington, DC, 1993. (b) Young, C. G.; Wedd, A. G. In ref 1a, p 70. (c) Enemark, J. H.; Young, C. G. *Adv. Inorg. Chem.* **1993**, *40,* 1 and references therein.
(2) Young, C. G.; Wedd, A. G. In *Encyclopedia of Inorganic Chemistry;* King, R. B., Ed.; Wiley: New York, 1994; p 2330 and references therein.
(3) Hille, R. *Chem. Rev.,* in press.
(4) (a) Chan, M. K.; Makund, W.; Kletzin, A.; Adams, M. W. W.; Rees, D. C. *Science* **1995**, *267,* 1463. (b) Ramao M. J.; Archer, M.; Moura, I.; Moura, J. J. G.; LeGall, J.; Engh, R.; Schneider, M.; Hof, P.; Huber, R. *Science* **1995**, *270,* 1170. (c) Schindelin, H.; Kisker, C.; Hilton, J.; Rajagopalan, K. V.; Rees D. C. *Science* **1996,** *272,* 1615.
(5) (a) Bray, R. C. *Adv. Enzymol. Relat. Areas Mol. Biol.* **1980**, *51,* 107. (b) Bray, R. C. *Q. Rev. Biophys.* **1988**, *21,* 299.
(6) Cohen, H. J.; Fridovich, I.; Rajagopalan, K. V. *J. Biol. Chem.* **1971**, *246,* 374.
(7) Adams, M. W. W; Mortenson, L. E. In *Molybdenum Enzymes*; Spiro, T. G., Ed.; Wiley: New York, 1985; p 519.

S0020-1669(96)01065-8 CCC: $12.00

experiments.[8] Recent studies of dimethyl sulfoxide reductase from *Rhodobacter sphaeroides* have provided direct experimental evidence for OAT processes in this enzyme.[9] EPR signals characteristic of oxo−Mo(V) centers have been closely examined for several molybdenum enzymes, and results are consistent with regeneration of the active site occurring via two one-electron processes (reactions 3 and 4), the first of which produces transient Mo(V) states.[5]

A goal of our research has been to develop a functional model that mimics all of the key reactions of the proposed enzyme catalytic cycle of Scheme 1. A number of model systems are known to carry out two-electron OAT processes that interconvert *cis*-$[Mo^{VI}O_2]^{2+}$ and $[Mo^{IV}O]^{2+}$ centers,[1−3,10,11] and coupled OAT processes have been used to catalytically oxidize tertiary phosphines using *N*-oxides and *S*-oxides. However, in general, such OAT systems do not exhibit one-electron processes and do not carry out steps 3 and 4 of Scheme 1. Transient *cis*-$[Mo^{V}O(OH)]^{2+}$ centers have been detected and characterized by EPR in solution by one-electron reduction of *cis*-$[Mo^{VI}O_2]^{+}$ complexes or one-electron oxidation of $[Mo^{IV}O]^{2+}$ complexes in wet solvents.[12−19] In the present work, interconversion of Mo(VI), Mo(V), and Mo(IV) has been examined in detail for the model system based upon $LMo^{VI}O_2X$ complexes [L = hydrotris(3,5-dimethylpyrazol-1-yl)borate; X = Cl, Br, NCS, OPh, SPh, SCH_2Ph, $SCHMe_2$]. Reactions 2−4 have been studied individually, and intermediates have been trapped and identified structurally and spectroscopically. The complexes catalyze multiple-turnover oxidations of tertiary phosphines to phosphine oxides, and oxygen isotope tracer experiments show that water is the source of the oxygen atom that becomes incorporated into the substrate. This model system incorporates all of the key reactivity features of Scheme 1 and many of the intermediates that have been proposed for enzymes containing $[Mo^{VI}O_2]^{2+}$ centers. Preliminary aspects of this catalytic cycle have been communicated and its energy profile and molecular mechanism examined theoretically.[15]

Experimental Section

Materials and Methods. Unless otherwise specified, all reactions and manipulations were carried out under an atmosphere of dinitrogen using standard Schlenk and glovebox techniques. Workups were generally performed in air without special precautions. The complexes $LMo^{VI}O_2X$ (X = Cl, Br, OPh, SPh, SCH_2Ph, $SCHMe_2$),[16,20] cobaltocene ($CoCp_2$; purified by repeated sublimation),[21] and $[FeCp_2][PF_6]$[22] were prepared according to literature methods. Chlorotrimethylsilane (Aldrich) was dried and distilled from $AlCl_3/CaH_2$. Triphenylphosphine (Aldrich) was recrystallized twice from CH_2Cl_2/*n*-hexane and dried at 65 °C in vacuum for 24 h. The solvents used for synthesis and electrochemical studies were dried and distilled under purified dinitrogen using literature methods.[23] The solvents employed for the isotope studies were further dried by stirring over alumina (dried at 200 °C for 24 h) for 12 h prior to immediate use. Water (95 atom % $H_2{}^{18}O$) was purchased from Aldrich Chemicals.

Infrared spectra were recorded on Perkin-Elmer 1430 and 1720X Fourier transform IR spectrophotometers as pressed KBr disks calibrated with polystyrene film. EPR spectra were obtained on a Varian E-9 spectrophotometer using 1,1-diphenyl-2-picrylhydrazyl as reference. ^1H and ^{31}P NMR spectra were recorded on a Varian Unity-300 spectrometer using $CHCl_3$ (internal, $\delta = 7.24$) and 85% H_3PO_4 (external, $\delta = 0$) as references. Mass spectrometric measurements were carried out on a Vacuum Generators Micromass 7070 F spectrometer operating at 70 eV in the EI mode. Electrochemical experiments were performed as described previously.[16] Potentials are quoted relative to the saturated calomel electrode (SCE). Microanalyses were performed by Atlantic Microlabs, Norcross, GA.

Syntheses. $LMoO^{IV}(SPh)(py)$. Method 1. A solution of $LMo^{VI}O_2(SPh)$ (0.10 g, 0.19 mmol) and PPh_3 (0.10 g, 0.38 mmol) in pyridine (6 mL) was stirred overnight and then evaporated to dryness under vacuum. The green product was purified by chromatography using $MeCN/CH_2Cl_2$ (1/20) as eluant and recrystallized from MeOH. Yield: 95 mg (85%). Anal. Calcd for $C_{26}H_{32}BMoN_7OS$: C, 52.27; H, 5.40; N, 16.41. Found: C, 52.38; H, 5.44; N, 16.56. Infrared: ν(B−H) 2543 m, ν(Mo═O) 939 s cm^{-1}. ^1H NMR ($CDCl_3$): δ 1.83 (3H), 1.94 (3H), 2.00 (3H), 2.35 (3H), 2.42 (3H), 2.49 (3H), 5.57 (1H), 5.75 (1H), 5.87 (1H), 6.58 (d, 2H, *J* 6.8 Hz, SPh), 6.72−6.80 (m, 3H, SPh), 7.45−7.82 (m, 4H, py), 8.61 (br, 1H, py). Electrochemistry (MeCN): Mo^V/Mo^{IV} +0.133 V (ΔE = 75 mV and I_a/I_c = 1.0 at a scan rate of 0.1 V·s^{-1}). ^{18}O-Labeled $LMo^{VI}O(SPh)(py)$ was prepared from ^{18}O-enriched $LMo^{VI}O_2(SPh)$.[18] Infrared: ν(B−H) 2543 m, ν(Mo═O) 895 s cm^{-1}.

Method 2. Green microcrystals of $[CoCp_2][LMo^{V}O_2(SPh)]$ precipitated rapidly upon addition of pyridine (6 mL) to a mixture of $LMo^{VI}O_2(SPh)$ (0.11 g, 0.20 mmol) and $CoCp_2$ (0.09 g, 0.46 mmol). The green crystals dissolved after stirring overnight at room temperature to form a yellow-green solution. The workup of method 1 provided a 51% yield of $LMo^{IV}O(SPh)(py)$.

$LMo^{IV}O(SR)(py)$ (R = CH_2Ph, $CHMe_2$). A procedure analogous to method 1 above was followed, but PBu^n_3 was used in place of PPh_3. The yields were 90 and 71% for R = CH_2Ph and $CHMe_2$, respectively. $LMo^{IV}O(SCH_2Ph)(py)$: infrared ν(B−H) 2539 m, ν(Mo═O) 949 s cm^{-1}; ^1H NMR ($CDCl_3$) δ 1.81 (3H), 1.84 (3H), 2.30 (3H), 2.39 (3H), 2.54 (3H), 2.76 (3H), 3.11 (d, 1H, ^2J 12.4 Hz, C*H*$_2$Ph), 3.81 (d, 1H, ^2J 12.4 Hz, C*H*$_2$Ph), 5.51 (1H), 5.84 (1H), 6.09 (1H), 6.87 (d, 2H, *J* 9.0 Hz, SPh), 6.89−7.06 (m, 3H, SPh), 7.4 (br, 2H, py), 7.66 (t, 1H, *J* 7.7 Hz, py), 8.1 (br, 1H, py), 9.1 (br, 1H, py); electrochemistry (MeCN) Mo^V/Mo^{IV} +0.033 V (ΔE = 91 mV and I_a/I_c = 1.0 at a scan rate of 0.1 V·s^{-1}). $LMo^{IV}O(SCHMe_2)(py)$: infrared ν(B−H) 2541 m, ν(Mo═O) 941 s cm^{-1}; ^1H NMR ($CDCl_3$) δ 0.48 (d, 3H, ^3J 6.7 Hz, CH*Me*$_2$), 1.37 (d, 3H, ^3J 6.7 Hz, CH*Me*$_2$), 1.84 (3H), 2.01 (3H), 2.27 (3H), 2.36 (3H), 2.52 (3H), 2.64 (3H), 3.02 (septet, 1H, ^3J 6.7 Hz, C*H*Me$_2$), 5.28 (1H), 5.53 (1H), 5.81 (1H), 7.43 (br, 2H, py), 7.69 (t, 1H, *J* 7.6 Hz, py), 8.1 (br, 1H, py), 9.2 (br, 1H, py); electrochemistry (MeCN) Mo^V/Mo^{IV} +0.014 V (ΔE = 84 mV and I_a/I_c = 1.0 at a scan rate of 0.1 V·s^{-1}).

Reaction of $LMo^{IV}O(SPh)(py)$ and Me_2SO. Dimethyl sulfoxide (0.32 mL, 4.68 mmol) was added to a solution of $LMo^{IV}O(SPh)(py)$

(8) Hille, R.; Sprecher, H. *J. Biol. Chem.* **1987**, *262*, 10914.
(9) Schultz, B. E.; Hille, R.; Holm, R. H. *J. Am. Chem. Soc.* **1995**, *117*, 827.
(10) (a) Holm, R. H.; Berg, J. M. *Acc. Chem. Res.* **1986**, *19*, 363. (b) Holm, R. H. *Chem. Rev.* **1987**, *87*, 1401. (c) Holm, R. H. *Coord. Chem. Rev.* **1990**, *110*, 183.
(11) (a) Gheller, S. F.; Schultz, B. E.; Scott, M. J.; Holm, R. H. *J. Am. Chem. Soc.* **1992**, *114*, 6934. (b) Schultz, B. E.; Gheller, S. F.; Muetterties, M. C.; Scott, M. J.; Holm, R. H. *J. Am. Chem. Soc.* **1993**, *115*, 2714. (c) Schultz, B. E.; Holm, R. H. *Inorg. Chem.* **1993**, *32*, 4244.
(12) Dowerah, D.; Spence, J. T.; Singh, R.; Wedd, A. G.; Wilson, G. L.; Farchione, F.; Enemark, J. H.; Kristofzski, J.; Bruck, M. *J. Am. Chem. Soc.* **1987**, *109*, 5655.
(13) Wilson, G. L.; Greenwood, R. J.; Pilbrow, J. R.; Spence, J. T.; Wedd, A. G. *J. Am. Chem. Soc.* **1991**, *113*, 6803.
(14) Greenwood, R. J.; Wilson, G. L.; Pilbrow, J. R.; Wedd, A. G. *J. Am. Chem. Soc.* **1993**, *115*, 5385.
(15) (a) Xiao, Z.; Young, C. G.; Enemark, J. H.; Wedd, A. G. *J. Am. Chem. Soc.* **1992**, *114*, 9194. (b) Pietsch, M. A.; Hall, M. B. *Inorg. Chem.* **1996**, *35*, 1273.
(16) Xiao, Z.; Bruck, M. A.; Doyle, C.; Enemark, J. H.; Grittini, C.; Gable, R. W.; Wedd, A. G.; Young, C. G. *Inorg. Chem.* **1995**, *34*, 5950.
(17) Xiao, Z.; Gable, R. W.; Wedd, A. G.; Young, C. G. *J. Chem. Soc., Chem. Commun.* **1994**, 1295.
(18) Xiao, Z.; Gable, R. W.; Wedd, A. G.; Young, C. G. *J. Am. Chem. Soc.* **1996**, *118*, 2912.
(19) Laughlin, L. J.; Young, C. G. *Inorg. Chem.* **1996**, *35*, 1050.
(20) Roberts, S. A.; Young, C. G.; Kipke, C. A.; Cleland, W. E., Jr.; Yamanouchi, K.; Carducci, M. D.; Enemark, J. H. *Inorg. Chem.* **1990**, *29*, 3650.
(21) (a) Wilkinson, G.; Cotton, F. A.; Birmingham, J. M. *J. Inorg. Nucl. Chem.* **1956**, *2*, 95. (b) King, R. B. *Organomet. Synth.* **1965**, *1*, 70.
(22) Desbois, M.-H.; Astruc. D. *New J. Chem.*, **1989**, *13*, 595.
(23) Perrin, D. D.; Armarego, W. L. F.; Perrin, D. R. *Purification of Laboratory Chemicals;* 2nd ed.; Pergamon Press: Oxford, U.K., 1980.

(70 mg, 0.117 mmol) in toluene (10 mL). After being stirred at 40 °C for 24 h, the solution was evaporated to dryness under vacuum and the residue chromatographed on silica gel using dichloromethane as eluant. The first dark-brown fraction was collected and the solid recrystallized from CH_2Cl_2/MeOH. ^{1}H NMR and IR spectra identified the product as $LMo^{VI}O_2(SPh)$.[16] Yield: 53 mg (85%).

Generation of EPR Signals in Solution. (i) $LMo^{V}O(OH)X$. $LMo^{VI}O_2X$ was dissolved in a solution of PPh_3 or PBu^n_3 in water-saturated toluene or THF (1−2 M H_2O). The intensity of the EPR signal reached a maximum in 10−30 min. Provided PPh_3 is present in excess, the spectra produced are essentially the same under either aerobic or anaerobic conditions.

(ii) $[LMo^{V}O(SR)(py)]^+$. To a mixture of $LMo^{IV}O(SR)(py)$ (R = Ph, CH_2Ph, $CHMe_2$) and $[FeCp_2][PF_6]$ was added dry MeCN/THF (1/9, v/v) and the solution transferred to an EPR tube under anaerobic conditions.

Reactions of $LMo^{VI}O_2X$ and PPh_3 in Dry Solvents. Previous work[15,20] has shown that inner sphere OAT reactions involving $LMo^{VI}O_2X$ and PPh_3 in dry solvents lead to intermediates which behave as coordinatively-unsaturated $LMo^{IV}OX$ or weakly solvated $LMo^{IV}OX$(solvent). Further investigations using $LMo^{VI}O_2$(SPh) and PPh_3 (Mo/P < 1) have been carried out under rigorously anaerobic conditions in solvents exhaustively dried over activated alumina.

(i) Toluene or THF. Reaction produced a dark purple-brown mixture containing at least six products according to thin-layer chromatography (TLC). The major product, isolated in 13% yield only, was $[LMo^{V}O(SPh)]_2(\mu$-O),[24] plausibly produced by comproportionation:

$$LMo^{IV}O(SPh) + LMo^{VI}O_2(SPh) \rightarrow [LMo^{V}O(SPh)]_2(\mu\text{-O}) \quad (5)$$

EPR spectroscopy detected at least two Mo(V) species in the reaction mixture, the major component being $LMo^{V}O(SPh)_2$.[25]

(ii) Dichloromethane. At least four different products were detected by TLC. The complexes $LMo^{V}OCl(SPh)$ (52%; plausibly formed by chlorine atom extraction from the solvent by the Mo(IV) intermediate) and $[LMo^{V}O(SPh)]_2(\mu$-O) (<10%; see eq 5) were isolated in substance. For X = Cl, the reaction appeared to be cleaner, with $LMo^{V}OCl_2$ being isolated in >90% yield.[20] However, the presence of water and O_2 disfavored the formation of $[LMo^{V}OCl]_2(\mu$-O) and increased the yield of $LMo^{V}OCl_2$ (vide infra).

(iii) Methanol. The reaction produced a dark-green solution in MeOH/THF (1/9 v/v). Two EPR signals were detected; their *g* and *A* values identified the compounds as $LMo^{V}O(OMe)(SPh)$ and $LMo^{V}O(OH)(SPh)$.[16,26]

(iv) Pyridine. The initial dark-brown solution turned yellow-green over 5 h. The only molybdenum-containing product detected by TLC was $LMo^{IV}O(SPh)(py)$. It was isolated in substance in 85% yield. No EPR signal was detected in the yellow-green solution produced using pyridine/THF (1/9 v/v) as the reaction medium. Reaction of $LMo^{IV}O(SPh)(py)$ with Me_2SO produced $LMo^{VI}O_2(SPh)$ in 85% isolated yield.

Reactions of $LMo^{VI}O_2X$ and PPh_3 in Wet Solvents. (i) Toluene or THF. Under anaerobic conditions, the initial product solutions were green, not dark purple-brown as observed under anhydrous conditions. They featured clean, intense EPR signals exhibiting the ^{1}H coupling characteristic of $LMo^{V}O(OH)X$.[16] The final major product after workup in air was the starting complex $LMo^{VI}O_2X$. For X = SPh, the recovery was 90%. The stability of the green solution was dependent on the amount of water present and the nature of ligand X. Higher concentrations of water (1−3 M) in THF favored the green solution. The color persisted longer in THF than in toluene presumably due to the limited solubility of water in toluene. For bulky X, such as SPh, the solutions remained green and exhibited the intense EPR signal of $LMo^{V}O(OH)(SPh)$ even after 20 h. For smaller and/or more labile X (e.g., Cl or Br), the green solutions were less stable and, in toluene, turned dark purple-brown after a few hours, becoming EPR-silent or producing unknown EPR-active Mo(V) species.

(ii) Dichloromethane. Under anaerobic and water-saturated conditions, the initial EPR signal was that of $LMo^{V}O(OH)(SPh)$. Upon standing, the signal assigned to $LMo^{V}OCl(SPh)$[25] increased in intensity. Under aerobic conditions with excess PPh_3, the signal for $LMo^{V}O(OH)(SPh)$ diminished rapidly while the signal for $LMo^{V}OCl(SPh)$ intensified as the system cycled catalytically (vide infra). Finally, $LMo^{V}OCl(SPh)$ was trapped as the major product (detected by EPR and TLC)

(iii) Methanol/THF. When $LMo^{VI}O_2(SPh)$ reacted in H_2O/MeOH/THF (1/1/18 v/v/v) under anaerobic conditions, two overlapping EPR signals assigned to $LMo^{V}O(OH)(SPh)$ and $LMo^{V}O(OMe)(SPh)$ were observed. Upon exposure to O_2, the former signal decayed rapidly while the latter increased in intensity. When the reaction was carried out with excess PPh_3 in methanol (AR grade) in air, the dark green complex $LMo^{V}O(OMe)(SPh)$ was isolated in 85% yield.[26]

(iv) Pyridine/THF. When $LMo^{VI}O_2X$ (X = SPh, Cl) reacted in H_2O/py/THF (1/1/8 v/v/v), the EPR signal intensity of $LMo^{V}O(OH)X$ was <5% of that generated under the same conditions in the absence of pyridine. Stable $LMo^{IV}OX(py)$ was the major product.

Catalytic Oxidation of PPh_3. (i) By $LMo^{VI}O_2(SPh)$. Tetrahydrofuran (15 mL) and water (0.14 mL, 7.8 mmol) were added to a mixture of $LMo^{VI}O_2(SPh)$ (50 mg, 0.094 mmol) and PPh_3 (1.30 g, 4.96 mmol). The purple-brown solution was stirred at 25 °C with constant bubbling of solvent-saturated dioxygen through the solution. The reaction was monitored by TLC (silica gel and 1/3 n-C_5H_{12}/CH_2Cl_2), which indicated that PPh_3 was converted quantitatively to $OPPh_3$ in *ca.* 20 h, i.e., about 50 turnovers under these conditions. At 40 °C, 100 such turnovers were achieved in *ca.* 10 h and the rate was increased 4-fold. After reaction, the solution was evaporated to dryness and the residue chromatographed on a silica gel column. Following elution of a trace of PPh_3 with *n*-hexane/toluene (1/1 v/v), dichloromethane was used to elute the dark-brown $LMo^{VI}O_2(SPh)$ and THF was used to elute $OPPh_3$. Evaporation of the eluted $OPPh_3$ solution to dryness under vacuum produced 1.34 g of solid $OPPh_3$ (97%) identical to an authentic sample (ν(P═O) 1190 s cm^{-1}; mp: 154−157 °C).[27] The process was also monitored by ^{31}P NMR: a small aliquot of sample was removed from the mixture during the course of reaction and the ^{31}P NMR spectrum recorded immediately.

(ii) By $LMo^{VI}O_2Cl$. At 15 °C, the same procedure as above allowed $LMo^{VI}O_2Cl$ (21 mg, 0.046 mmol) to convert 100 equiv of PPh_3 (1.23 g, 4.72 mmol) into $OPPh_3$ in *ca.* 10 h.

Oxygen Atom Tracer Studies. (i) Reaction of $LMo^{16}O_2(SPh)$ with PPh_3 in $H_2{}^{18}O$/Pyridine. To a mixture of $LMo^{16}O_2(SPh)$ (0.16 g, 0.30 mmol) and PPh_3 (0.04 g, 0.15 mmol) were added $H_2{}^{18}O$ (95 atom % ^{18}O; 0.07 mL, 3.5 mmol) and alumina-dried pyridine (3 mL). After the reaction mixture was stirred for 6 h, the products $LMo^{IV}O(SPh)(py)$ and $OPPh_3$ were isolated, and both were found to contain less than 5 atom % ^{18}O. Incorporation of an oxygen atom from the $[Mo^{VI}O_2]^{2+}$ center to PPh_3 was 95% efficient as assessed by EI-MS.[28a]

(ii) Reaction of $LMo^{18}O_2(SPh)$ with PPh_3 in $H_2{}^{16}O$/Pyridine. Pyridine (2 mL) containing 0.2 mL of $H_2{}^{16}O$ was added to a mixture of $LMo^{18}O_2(SPh)$ (85 atom % ^{18}O; 20 mg, 0.037 mmol) and PPh_3 (10 mg, 0.038 mmol). After the reaction mixture was stirred for 6 h, the products $LMo^{IV}O(SPh)(py)$ and $OPPh_3$ were isolated. The content of ^{18}O label in both products was 70 atom %. Incorporation of an oxygen atom from the $[Mo^{VI}O_2]^{2+}$ center to PPh_3 was about 80% efficient.[28b]

(iii) Reaction of $LMo^{16}O_2X$ with PPh_3 in $H_2{}^{17}O$/THF. Triphenylphosphine (0.02 g, 0.076 mmol) and $H_2{}^{17}O$ (51.2 atom % ^{17}O; 0.03 mL, 1.6 mmol) were dissolved in active alumina-dried THF (1.5 mL). An aliquot of this solution (*ca.* 0.3 mL) was transferred anaerobically into an EPR tube containing $LMo^{VI}O_2X$ (X = Cl, Br, OPh, SCH_2Ph, SPh; *ca.* 1 mg), and the reaction monitored by

(24) Xiao, Z.; Enemark, J. H.; Wedd, A. G.; Young C. G. *Inorg. Chem.* **1994**, *33*, 3438.
(25) Cleland, W. E., Jr.; Barnhart, K. M.; Yamanouchi, K.; Collison, D.; Mabbs, F. E.; Ortega, R. B.; Enemark, J. H. *Inorg. Chem.* **1987**, *26*, 1017.
(26) Xiao, Z.; Bruck, M. A.; Enemark, J. H.; Young, C. G.; Wedd, A. G. *J. Biol. Inorg. Chem.* **1996**, *1*, 415.
(27) *Dictionary of Organic Compounds*, 5th ed.; Chapman and Hall: New York, 1982; Vol. 5, p 5618.
(28) (a) Incorporation efficiency IE = (% ^{16}O in $OPPh_3$ − % ^{16}O from H_2O)/(% ^{16}O in $[MoO_2]$), where % ^{16}O from H_2O = % ^{16}O in H_2O × (% ^{18}O in $OPPh_3$/% ^{18}O in H_2O). (b) IE = (% ^{18}O in $OPPh_3$ − % ^{18}O from H_2O)/(% ^{18}O in $[MoO_2]$).

Table 1. Crystallographic Data for $LMo^{IV}O(SPh)(py)\cdot 0.6MeOH$

formula	$C_{26.6}H_{34.4}BMoN_7O_{1.6}S$	Z	8
color	dark green	space group	*Pbca*
fw	616.64	ρ, g·cm^{-3}	1.40
a, Å	13.790(2)	μ, cm^{-1}	5.3
b, Å	15.266(2)	*R*	0.048
c, Å	27.807(5)	R_w	0.061
V, Å^3	5853(3)		

EPR. Control experiments with $H_2{}^{16}O$ (100 atom % ^{16}O) were conducted under the same conditions.

(iv) Reaction of $LMo^{16}O_2(SPh)$ with PPh_3 in $H_2{}^{18}O$/THF. The anaerobic reaction of $LMo^{16}O_2(SPh)$ (0.40 g, 0.75 mmol), PPh_3, and H_2O (95 atom % ^{18}O) in the molar ratio 2.2/1/36 in active alumina-dried THF produced a dark-green solution which was stirred for 7 h. Bubbling of O_2 through the solution regenerated the initial dark-brown color, and the product $LMo^{VI}O_2(SPh)$ (80−85 atom % ^{18}O) was isolated in 72% yield.[18] The $OPPh_3$ coproduct was isolated and recrystallized from CH_2Cl_2/*n*-hexane. Its infrared spectrum revealed absorptions corresponding to $\nu(P^{16}O)$ and $\nu(P^{18}O)$ at 1190 and 1153 cm^{-1}, respectively, while EI-MS confirmed the presence of 36 atom % ^{18}O.[29]

(v) Reaction of $LMo^{18}O_2(SPh)$ with PPh_3 in $H_2{}^{16}O$/THF. Under anaerobic conditions, $H_2{}^{16}O$/THF (1/4 v/v; 1 mL) which had been deoxygenated by three freeze−pump−thaw cycles was added to a mixture of $LMo^{18}O_2(SPh)$ (85 atom %; 18 mg, 0.034 mmol) and PPh_3 (1 mg, 0.0038 mmol) (Mo/P = 9/1). After the purple-brown solution was stirred for 7 h, $^{16}O_2$ was bubbled through the solution, and $LMo^{VI}O_2(SPh)$ was isolated. The ^{18}O label in $LMo^{VI}O_2(SPh)$ was diluted to 55%, and its infrared spectrum showed a high $^{16}O^{18}O$ isotopomer content.

(vi) Reaction of $LMo^{16}O_2(SPh)$ with PPh_3 and $^{16}O_2$ in $H_2{}^{18}O$/THF. A mixture of $H_2{}^{18}O$ (95 atom % ^{18}O; 156 μL, 7.8 mmol) and dry THF (4 mL) was introduced into a Schlenk flask containing a mixture of $LMo^{VI}O_2(SPh)$ (0.21 g, 0.39 mmol) and PPh_3 (0.30 g, 1.15 mmol) under an atmosphere of dry $^{16}O_2$. The reaction mixture was stirred vigorously for 3 h under a positive pressure of $^{16}O_2$ and retained the dark-brown color of the starting material $LMo^{VI}O_2(SPh)$. The products $LMo^{VI}O_2(SPh)$ (0.19 g; yield 90%) and $OPPh_3$ (0.31 g; yield, 97%) incorporated 55 and 16 atom % ^{18}O, respectively.[29]

Crystal Structure Determination. Crystals of $LMo^{IV}O(SPh)(py)\cdot 0.6MeOH$ were grown by refrigeration of a saturated solution in methanol at *ca.* −15 °C for several days. Crystallographic data are listed in Table 1, and positional parameters, in the Supporting Information. Preliminary examination and data collection were performed with Mo K$\bar{\alpha}$ radiation (λ = 0.710 73 Å) on a Syntex $P2_1$ diffractometer. Accurate cell parameters were obtained from least-squares refinement of the setting angles of 30 reflections in the range $15 < 2\theta < 30°$. Three reflections monitored every 97 reflections during X-ray exposure time showed no intensity variation. The data were corrected for Lorentz and polarization effects but not for absorption. Neutral-atom scattering factors were taken from the literature, the values being corrected for anomalous dispersion.[30] The structure was solved by using a combination of Patterson and difference electron density syntheses. The full-matrix least-squares refinement defined anisotropic temperature factors for each of the non-hydrogen atoms; hydrogen atoms were included with fixed isotropic temperature factors and coordinates constrained by the riding model. Analysis of variance after final refinements showed no unusual features. All calculations were performed using Mo1EN software.[31]

Results and Discussion

Characterization of New Complexes. The infrared spectra of $LMo^{IV}O(SR)(py)$ (R = Ph, CH_2Ph, $CHMe_2$) each exhibited a strong band in the range 950−930 cm^{-1}. Its assignment to the ν(Mo═O) vibration was supported by ^{18}O-labeling of $LMo^{IV}O(SPh)(py)$ (Experimental Section). Bands characteristic of L and the thiolate and pyridine coligands were also evident. ^1H NMR spectra of the complexes show that all methyl and methine groups of L are inequivalent, with six singlet methyl resonances (3/3/3/3/3/3 integration) and three singlet methine resonances (1/1/1 integration). The two methylene hydrogens for R = CH_2Ph ligand are diastereotopic, and geminal coupling was observed. The large chemical shift difference between these two hydrogens (210 Hz) is attributed to differential ring current effects of the pyridine ligand. The two diastereotopic methyl groups for R = $CHMe_2$ also resonate at quite different frequencies for the same reason.

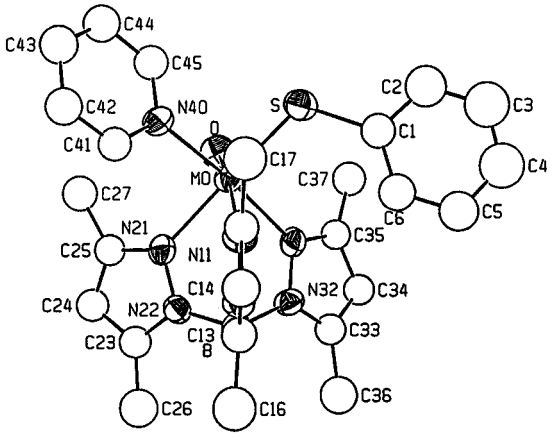

Figure 1. Molecular structure of $LMo^{IV}O(SPh)(py)$ showing the atom-labeling scheme. The labeling of the ring pyrazole containing N(11) and N(31) follows that shown for the ring containing N(21). Hydrogen atoms are omitted for clarity.

Table 2. Bond Distances and Angles for $LMo^{IV}O(SPh)(py)$

Distances (Å)					
Mo−O	1.667(5)	Mo−S	2.390(3)	Mo−N(40)	2.184(5)
Mo−N(11)	2.375(6)	Mo−N(21)	2.194(7)	Mo−N(31)	2.144(6)
S−C(1)	1.755(9)				

Angles (deg)			
O−Mo−S	103.3(2)	O−Mo−N(40)	95.9(2)
O−Mo−N(11)	169.7(3)	O−Mo−N(21)	92.0(3)
O−Mo−N(31)	93.9(2)	S−Mo−N(40)	84.6(2)
S−Mo−N(11)	86.5(2)	S−Mo−N(21)	164.2(2)
S−Mo−N(31)	97.0(2)	N(40)−Mo−N(11)	88.2(2)
N(40)−Mo−N(21)	89.7(2)	N(40)−Mo−N(31)	169.4(2)
N(11)−Mo−N(21)	78.5(2)	N(11)−Mo−N(31)	81.4(2)
N(21)−Mo−N(31)	86.0(2)	Mo−S−C(1)	115.6(3)

The complex $LMo^{IV}O(SPh)(py)$ was further characterized by an X-ray structure analysis. The molecular structure and atom-labeling scheme are shown in Figure 1, and selected bond distances and angles are listed in Table 2. The ligands are arranged in a distorted-octahedral geometry with a local C_1 symmetry. The three monodentate ligands are constrained to be mutually *cis* by the *fac* stereochemistry of L. The Mo═O bond distance is 1.667(5) Å, as expected for a six-coordinate oxo−Mo(IV) species.[32] The Mo−N(11) bond is significantly longer than other two Mo−N bonds due to the strong *trans* influence of the oxo ligand. The short Mo−N(31) bond *trans* to N(40) reflects the weak *trans* influence of pyridine ligand. Similar comments concerning the Mo−N distances apply to the previously characterized complex $LMo^{IV}OCl(py)$.[20] The average Mo−N bond in $LMo^{IV}O(SPh)(py)$ (2.238 Å) is 0.02 Å shorter than that in $LMoO_2(SPh)$ (2.257 Å).[16] The Mo−S bond

(29) EI-MS peaks for $[OPPh_3]^+$: 100 atom % ^{16}O sample, *m*/*z* (%) 277 (100), 278 (46.1), 279 (8.4); ^{18}O-enriched sample, *m*/*z* (%) 277 (100), 278 (54.4), 279 (64.0), 280 (29.6), 281 (4.8). The ^{18}O content in $OPPh_3$ was calculated from the relative intensity (*I*) at *m*/*z* = 279 (corrected) and 277: % $^{18}O = (I_{279} - 8.4\%\ I_{277})/[(I_{279} - 8.4\%\ I_{277}) + I_{277}]$.

(30) *International Tables for X-Ray Crystallography*; Kynoch: Birmingham, U.K., 1974; Vol. IV, pp 99, 149.

(31) *MolEN: An Interactive Structure Solution Procedure;* Enraf-Nonius: Delft, The Netherlands, 1990.

(32) Young, C. G.; Roberts, S. A.; Ortega, R. B.; Enemark, J. H. *J. Am. Chem. Soc.* **1987**, *109*, 2938.

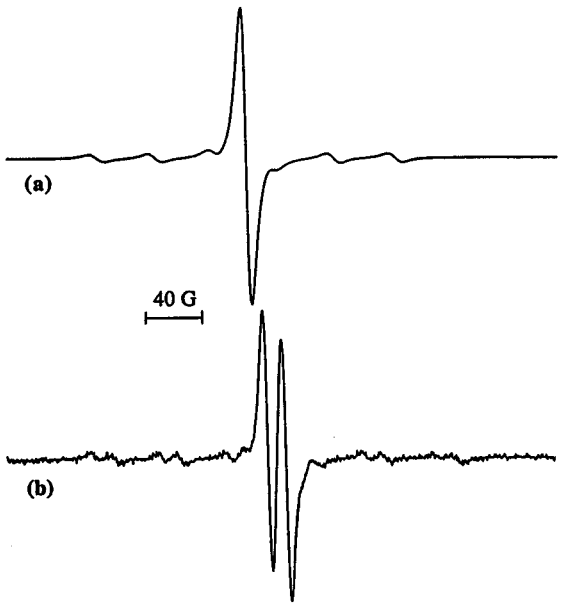

Figure 2. Room-temperature EPR spectra of (a) $[LMo^{V}O(SPh)(py)]^{+}$ generated in THF by ferrocenium oxidation of $LMo^{IV}O(SPh)(py)$ and (b) $LMo^{V}O(OH)(SPh)$ generated by addition of H_2O to solution (a).

in LMoO(SPh)(py) (2.390(3) Å) is shorter than that in $LMoO_2$(SPh) (2.402(2) Å).[16] A decrease in Mo−S bond length is also seen in dimethyl sulfoxide reductase upon loss of an oxo ligand from the monooxo−Mo(VI) form (Mo−S 2.43 Å) to the desoxo−Mo(V) form (Mo−S 2.40 Å).[33] The geometry of the LMoO fragment is similar to that found in $LMo^{V}O(SPh)_2$.[25] A comparison of the structures of $LMo^{IV}O(SPh)(py)$, $LMo^{V}O(SPh)_2$,[25] and $LMo^{VI}O_2(SPh)$[16] shows that the steric protection of the Mo=O unit(s) by the thiophenolate ligands is controlled to some extent by the coligands: when the coligand does not provide a steric barrier, the thiophenolate orients over the Mo=O ligand(s) (cf $LMo^{VI}O_2(SPh)$); when X is sterically bulky, the thiophenolate projects into a cleft between two pyrazole rings of L [cf $LMo^{IV}O(SPh)(py)$ and $LMo^{V}O(SPh)_2$].

$LMo^{IV}O(SR)(py)$ complexes exhibit well-defined oxidation processes with electrochemical parameters (see Experimental Section) compatible with the following couple:

$$[LMo^{V}O(SR)(py)]^{+} + e^{-} = LMo^{IV}O(SR)(py) \qquad (6)$$

Although the oxidation potentials of $LMo^{IV}O(SR)(py)$ (from 0 to +0.14 V *vs* SCE in MeCN) are sufficiently positive that the complexes are not oxidized by O_2, they are readily oxidized by the ferrocenium ion (+0.39 V), as evidenced by the ready development of a Mo(V) EPR signal in each case (Figure 2a). The signals may be assigned to the cationic species $[LMo^{V}O(SR)(py)]^{+}$ on the basis of comparison with related $[LMo^{V}O(S_2PR_2)]^{+}$ complexes (R = Me, Et, Pr^{i}, Ph).[19] The signals are observable in dry solvents only. Upon addition of H_2O, the initial signals are replaced rapidly by unstable proton-coupled signals (Figure 2b) identical to those assigned previously to air-sensitive $LMo^{V}O(OH)(SR)$ (Table 3):[16,18]

$$[LMo^{V}O(SR)(py)]^{+} + H_2O \rightarrow LMo^{V}O(OH)(SR) + pyH^{+} \qquad (7)$$

Attempts to prepare $LMo^{IV}O(OPh)(py)$ led to its isolation as a mixture with starting complex $LMo^{VI}O_2(OPh)$. Attempts to prepare other $LMo^{IV}O(OR)(py)$ complexes were unsuccessful.

(33) George, G. N.; Hilton, J.; Ragagopalan, K. V. *J. Am. Chem. Soc.* **1996**, *118*, 1113.

Table 3. EPR Parameters for $[LMoO(SR)(py)]^{+}$ and LMoO(OH)(SR) in THF

	$[LMoO(SR)(py)]^{+}$		LMoO(OH)(SR)		
R	$\langle g \rangle$	$\langle A(Mo) \rangle^{a}$	$\langle g \rangle$	$\langle A(Mo) \rangle^{a}$	$\langle A(H) \rangle^{a}$
Ph	1.962	38.0	1.953	43.2	11.7
CH_2Ph	1.964	38.7	1.953	42.3	10.5
$CHMe_2$	1.962	38.7	1.954	42.2	10.2

[a] Units: 10^{-4} cm^{-1}.

Scheme 2

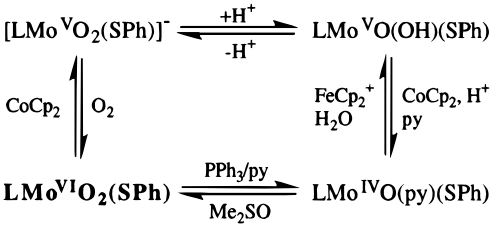

Such species would plausibly possess a more negative redox potential than $LMo^{IV}O(SR)(py)$ and be sensitive, especially in wet solvents, to aerial oxidation and hydrolysis during workup.

Oxygen Atom Transfer Reactions. The structurally characterized complexes $LMo^{VI}O_2(SPh)$[16] and $LMo^{IV}O(SPh)(py)$ are interconverted by PPh_3/py and Me_2SO (Scheme 2). Equivalent interconversions have been observed in closely-related systems, kinetics studies being consistent with inner-sphere oxygen atom transfer processes.[19,20,34] A number of other molybdenum systems have been examined in detail with the same conclusion.[10,11,35] An important aspect of such reactions is the electronic control exerted by the "spectator oxo" ligand in helping delocalize electron density during the reduction process.[36,37]

Coupled Electron−Proton Transfer Reactions. The one-electron reduction potential of the $LMo^{VI}O_2X$ complexes can be tuned to at least 0.5 V by variation of X.[16] In particular, this control led to isolation of $[CoCp_2][LMo^{V}O_2(SPh)]$ and the structural characterization of $[CoCp_2][L'Mo^{V}O_2(SPh)]$ [L′ = hydrotris(3,5-dimethyl-1,2,4-triazol-1-yl)borate] via use of the one-electron reductant $CoCp_2$.[17,18] Although $[L'Mo^{V}O_2(SPh)]^{-}$ does not readily protonate, $LMo^{V}O(OH)(SPh)$ was isolated as a coprecipitate with the conjugate base $[CoCp_2][LMo^{V}O_2(SPh)]$ (Scheme 2).[18] Neither form can be reduced voltammetrically in MeCN or pyridine at potentials up to −2.0 V vs SCE. However, the following reaction provides $LMo^{IV}O(SPh)(py)$ in 50% isolated yield:

$$LMo^{VI}O_2(SPh) + 2CoCp_2 + 2H^{+} + py \rightarrow LMo^{IV}O(SPh)(py) + 2[CoCp_2]^{+} + H_2O \qquad (8)$$

The one-electron-reduced intermediate $[CoCp_2][LMo^{V}O_2(SPh)]$ precipitates initially but slowly redissolves to complete the reaction. The second, slow, CEPT step is clearly driven by the high affinity of pyridine for the Mo(IV) center (Scheme 2). Reaction 7 allows the one-electron chemistry to be reversed and completed via oxidation of the Mo(V) species by O_2 (Scheme 2).

(34) Roberts, S. A.; Young, C. G.; Cleland, W. E., Jr.; Ortega, R. B.; Enemark, J. H. *Inorg. Chem.* **1988**, *27*, 3044.
(35) Das, S. K.; Chaudhury, P. P.; Biswas, D.; Sarkar, S. *J. Am. Chem. Soc.* **1994**, *116*, 9061.
(36) (a) Rappe, A. K.; Goddard, W. A., III. *Nature* **1980**, *285*, 311. (b) Rappe, A. K.; Goddard, W. A., III. *J. Am. Chem. Soc.* **1982**, *104*, 448.
(37) Belgacem, J.; Kress, J.; Osborn, J. A. *J. Am. Chem. Soc.* **1992**, *114*, 1501.

Scheme 3

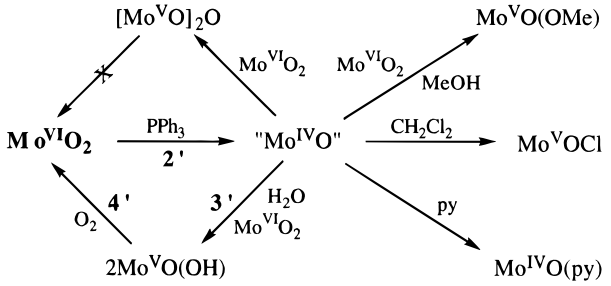

For clarity, ligands L and SPh are omitted from the formulae.

The present system allows interconversion of the structurally characterized species $LMo^{VI}O_2(SPh)$ and $LMo^{IV}O(SPh)(py)$ via **either** OAT or CEPT pathways and is the first one to do so.

Nature of the Mo(IV) State. The clean chemistry of Scheme 2 is dependent upon the presence of pyridine. However, Roberts et al.[20] investigated the reactions of $LMo^{VI}O_2X$ with PPh_3 in various solvents and found that the reaction stoichiometry and the nature of the molybdenum-containing products depend upon solvent. These observations were confirmed and extended in the present work employing rigorously dried solvents. In each case, the observed final products are consistent with a reactive intermediate, $LMo^{IV}OX$, that can be trapped as mononuclear Mo(IV), mononuclear Mo(V), or binuclear Mo(V), depending upon the system. Scheme 3 reports the major products observed for X = SPh. However, in the same but **wet** solvents, coordination of water appears to compete with the other processes

$$LMo^{IV}OX + H_2O \rightarrow LMo^{IV}OX(OH_2) \qquad (9)$$

The proposed intermediate $LMo^{IV}OX(OH_2)$ is oxidized rapidly to the EPR-active species $LMo^{V}O(OH)X$ via a comproportionation reaction involving Mo(VI) starting material:

$$LMo^{IV}OX(OH_2) + LMo^{VI}O_2X \rightarrow 2\,LMo^{V}O(OH)X \qquad (10\ (3'))$$

Overall, the present results indicate that effective competition for the available coordination site on $LMo^{IV}O(SPh)$ follows the order

$$\text{pyridine} > H_2O \sim \text{MeOH} > CH_2Cl_2 > [Mo^{VI}O_2]^{2+} > \text{THF} \sim \text{toluene} \qquad (11)$$

In wet THF or toluene, water competes effectively for the vacancy to yield $LMo^{V}O(OH)X$ (eqs 9 and 10) which can be oxidatively trapped by O_2 as the starting complex $LMo^{VI}O_2X$ in high yield (for X = Cl, 73%; for X = SPh, >90%).

The alternative product of comproportionation, $[LMo^{V}OX]_2(\mu\text{-O})$, is formed only in the absence of H_2O:

$$LMo^{IV}OX + LMo^{VI}O_2X \rightarrow [LMo^{V}OX]_2(\mu\text{-O}) \qquad (12)$$

Once formed, $[LMo^{V}OX]_2(\mu\text{-O})$ cannot be hydrolyzed under the conditions employed:

$$[LMo^{V}OX]_2(\mu\text{-O}) + H_2O \not\rightarrow 2\,LMo^{V}O(OH)X \qquad (13)$$

In THF containing both pyridine (~1 M) and water (~5 M), pyridine competes effectively for the vacancy (eq 11). Only a weak EPR signal of $LMo^{V}O(OH)X$ is observed. The intensity of the signal is *ca.* 1−5% of that generated under the same conditions without the addition of pyridine. In wet CH_2Cl_2 or MeOH, the solvent competes with water to produce $LMo^{V}OClX$ (via Cl atom transfer) or $LMo^{V}O(OMe)X$ (via comproportionation) as well as $LMo^{V}O(OH)X$ (Scheme 3). In the presence of excess PPh_3 in air, catalytic cycling of $LMo^{V}O(OH)X$ in these solvents leads to eventual trapping of all the molybdenum as the stable product $LMo^{V}OClX$ or $LMo^{V}O(OMe)X$.

Interestingly, when desulfoxanthine oxidase[38] and dimethyl sulfoxide reductase[33,39] are reduced in the presence of glycerol, stable Mo(V) EPR signals develop indicating that bound hydroxide on the Mo(V) centers appears to have been replaced by coordinated glycerol. The mechanism of formation of $LMo^{V}O(OMe)(SPh)$ may apply to these glycerol-inhibited Mo(V) forms in the enzymes.[26]

Catalytic Oxygen Atom Transfer. The reaction of $LMo^{VI}O_2X$ with PPh_3 in wet solvents produces $LMo^{V}O(OH)X$, which is oxidized rapidly to the starting complex upon admission of dioxygen (Scheme 3, reactions 2′−4′). The overall reaction appears to be

$$PPh_3 + H_2O + 2O_2 \rightarrow OPPh_3 + 2HO_2 \qquad (14)$$

Such a cycle is similar to that depicted in Scheme 1, reactions 2−4 with the first CEPT step 3′ being comproportionation reaction 10 and the second one being the oxidation

$$2LMo^{V}O(OH)X + 2O_2 \rightarrow 2LMo^{VI}O_2X + 2HO_2 \qquad (4')$$

In fact, the cycle is catalytic for $LMo^{VI}O_2X$ (X = Cl, SPh) in the presence of dioxygen and 0.5 M H_2O in THF: (i) At least 100 turnovers are possible with a 98% isolated yield of $OPPh_3$. The process can be monitored by TLC or ^{31}P NMR. No $OPPh_3$ is produced in the absence of the Mo complex. (ii) The observed catalytic rate is faster for X = Cl than for X = SPh. A rate of 0.2 min^{-1} is achieved at 15 °C for the Cl complex and at 40 °C for the SPh analogue. The catalysis is slow but persistent. The chemistry outlined in Schemes 2 and 3 allows detailed ^{18}O tracer studies of the present system. In particular, reactions 2′−4′ (Scheme 3) can be probed individually.

In other systems, transfer of the ^{18}O label between PEt_3 and $Mo^{VI}O_2(L{-}NS)_2$ and between Ph_2SO and $Mo^{IV}O(L{-}NS)_2$ (L−NS = bis(4-*tert*-butylphenyl)-2-pyridylmethanethiolate) has been demonstrated with 60% efficency, consistent with OAT.[11b] The enzyme dimethyl sulfoxide reductase has been examined in a similar way.[9] Reaction of $Mo^{VI}O_2(cys{-}OR)_2$ (cys−OR = cysteine ester), PPh_3, and $H_2{}^{18}O$ resulted in the appearance of the label in the product $OPPh_3$, but the mechanism of incorporation remains unclear.[40] Several other model systems appear to require O_2 and/or H_2O for regeneration of $[Mo^{VI}O_2]^{2+}$ from $[Mo^{IV}O]^{2+}$ centers.[41−47]

(38) Lowe, D. J.; Barker, M. J.; Pawlik, R. T.; Bray, R. C. *Biochem. J.* **1976**, *155*, 81.
(39) Finnegan, M. G.; Hilton, J.; Rajagopalan, K. V.; Johnson, M. K. *Inorg. Chem.* **1993**, *32*, 2616.
(40) Ueyama, N.; Yano, M.; Miyashita, H.; Nakamura, A.; Kamachi, M.; Nozakura, S. *J. Chem. Soc., Dalton Trans.* **1984**, 1447.
(41) Barral, R.; Bocard, C.; Roch, I. S.; Sajus, L. *Tetrahedron Lett.* **1972**, 1693.
(42) Newton, W. E.; Corbin, J. L.; Bravard, D. C.; Searles, J. E.; McDonald, J. W. *Inorg. Chem.* **1974**, *13*, 100.
(43) McDonald, D. B.; Shulman, J. I. *Anal. Chem.* **1975**, *47*, 2023.
(44) Chen, G. J.-J.; McDonald, J. W.; Newton, W. E. *Inorg. Chem.* **1976**, *15*, 2612.
(45) Durant, R.; Garner, C. D.; Hyde, M. R.; Mabbs, F. E. *J. Chem. Soc., Dalton Trans.* **1977**, 955.
(46) Speier, G. *Inorg. Chim. Acta* **1979**, *32*, 139.
(47) Cervilla, A.; Corma, A.; Fornés, V.; Llopis, E.; Pérez, F.; Rey, F.; Ribera, A. *J. Am. Chem. Soc.* **1995**, *117*, 6781.

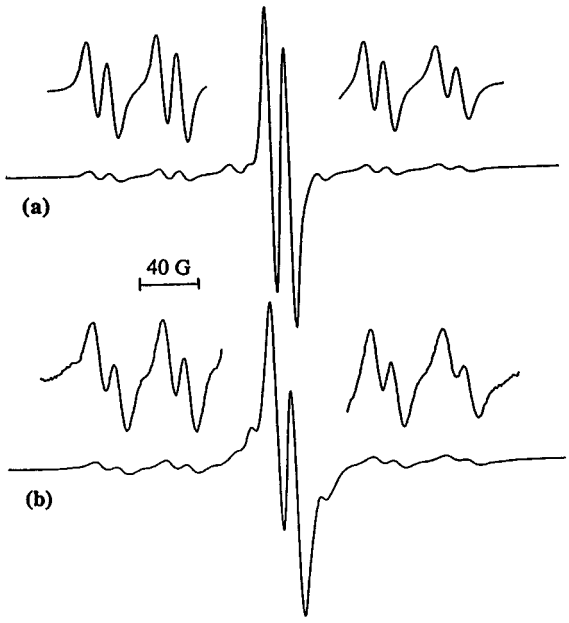

Figure 3. EPR spectra of LMoO(OH)(SPh) generated by reduction of $LMoO_2(SPh)$ with PPh_3 for 3 h at 293 K: (a) in THF/1 M $H_2{}^{16}O$; (b) in THF/1 M $H_2{}^{17}O$ (51.5 atom %).

Exchange of Oxygen between $[Mo^{VI}O_2]^{2+}$ Centers and H_2O. A number of $[Mo^{VI}O_2]^{2+}$ complexes exchange oxygen with H_2O but do not undergo reversible one-electron reduction.[11b,48−51] Others such as $MoO_2(L-N_2S_2)$ [$L-N_2S_2$ = dianion of *N*,*N*′-dimethyl-*N*,*N*′-bis(2-sulfanylphenyl)ethylenediamine] and $L''MoO_2(SPh)$ [L'' = hydrotris(3-isopropylpyrazol-1-yl)borate] exhibit the latter property but do not exchange oxygen with water.[13,18] The complex $LMo^{18}O_2(SPh)$ loses no label after incubation in $H_2{}^{16}O$/THF (1/4 v/v) in air for 24 h and so belongs to the second class. Similar experiments show that $LMo^{IV}O(SPh)(py)$ does not exchange oxygen with water.

Reaction 2′. In the present system, pyridine competes strongly with H_2O at the Mo(IV) level (eq 11). Suitable conditions allow effective blocking of reaction 3′. Mixing of $LMo^{16}O_2(SPh)$, PPh_3 and $H_2{}^{18}O$ (2/1/22) in pyridine produced $^{16}OPPh_3$ with 95% efficiency. The complementary reaction of $LMo^{18}O_2(SPh)$, PPh_3, and $H_2{}^{16}O$ (1/1/300) in pyridine produced $^{18}OPPh_3$ with 80% efficiency. The higher proportions of PPh_3 and H_2O in the second experiment presumably allow some conversion of Mo^{IV} to $LMo^{V}O(OH)(SPh)$ and subsequent leakage of label (*vide infra*: eqs 15 and 16). These two experiments unambiguously confirm transfer of oxygen from $LMoO_2(SPh)$ to PPh_3 in reaction 2 with minimal contribution from solvent H_2O.

Reactions 3′ and 4′. Scheme 3 indicates that reaction under anaerobic conditions will terminate after reaction 3′. The presence of excess PPh_3 in $H_2{}^{16}O$ (1 M)/THF allowed full development of the EPR intensity of $LMo^{V}O(OH)X$ (X = Cl, Br, OPh, SCH_2Ph, SPh) within 15 min. In systems containing $H_2{}^{17}O$ (51.5 atom % ^{17}O; $I = {}^5/_2$), initial spectra were indistinguishable from the $H_2{}^{16}O$ system, but full development of ^{17}O hyperfine coupling occurred within 3 h for X = OPh, SCH_2Ph, and SPh (Figure 3; cf refs 13, 14, and 52). For the less sterically protected systems $LMo^{V}O(OH)X$ (X = Cl, Br),

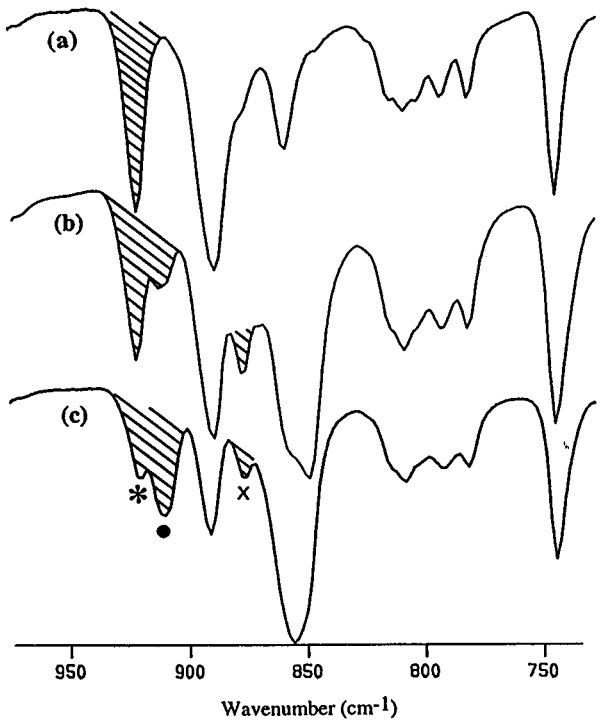

Figure 4. Infrared spectra of $LMoO_2(SPh)$ (KBr): (a) 100 atom % ^{16}O; (b) 55 atom % ^{18}O obtained by mixing 85 atom % ^{18}O and 100 atom % ^{16}O samples; (c) 55 atom % ^{18}O obtained by incubation of an 85 atom % ^{18}O sample with PPh_3 (9/1 mole ratio) in wet THF (20% $H_2{}^{16}O$). The $\nu_s(Mo^{VI}O_2)$ bands are shaded, and peaks *, ●, and × are assigned to the $\nu_s(Mo^{VI}O_2)$ modes of the $^{16}O^{16}O$, $^{16}O^{18}O$, and $^{18}O^{18}O$ isotopomers, respectively.

the coupling appeared within 1 h. Scheme 3 indicates that only $0.25 \times 51.5 = 13$ atom % ^{17}O label should appear in the $LMo^{V}O(OH)X$ product under anaerobic conditions due to reactions 2′ + 3′. It is apparent that $LMo^{V}O(OH)X$ exchanges oxygen with H_2O:

$$LMo^{16}O(^{16}OH)X + 2H_2{}^{17}O \rightleftharpoons LMo^{17}O(^{17}OH)X + 2H_2{}^{16}O \quad (15)$$

$LMo^{16}O_2(SPh)$, PPh_3, and $H_2{}^{18}O$ (95 atom % ^{18}O) in single-turnover proportions (2.2/1/36) were incubated for 7 h in THF under anaerobic conditions. Exposure to $^{16}O_2$ generated $LMoO_2$-(SPh) (>80 atom % ^{18}O). The content predicted in the absence of equilibrium 15 is $0.25 \times 95 = 24$ atom % ^{18}O. This single-turnover experiment also produced $OPPh_3$ (36 atom % ^{18}O). Scheme 3 (reaction 2′) predicts no ^{18}O content, and incubation of $^{18}OPPh_3$ in $H_2{}^{16}O$/THF (1/5 v/v) showed no exchange over 3 days. Although $LMo^{VI}O_2(SPh)$ does not undergo exchange with water, the simple H atom transfer[53] equilibrium 16 connects

$$Mo^{VI}O_2 + Mo^{V}O(^{18}OH) \rightleftharpoons Mo^{V}O(OH) + Mo^{VI}O^{18}O \quad (16)$$

the Mo^{VI} and Mo^{V} states. Under nominal single-turnover conditions with reaction 2′ as the rate-determining step, equilibrium 16 allows multiple turnovers for some Mo centers, leading to leakage of label into the product $OPPh_3$.

$LMo^{18}O_2(SPh)$ (85 atom % ^{18}O), PPh_3, and $H_2{}^{16}O$ in THF were incubated anaerobically in proportions 9/1/3000. According to Scheme 3, the final ratio $LMo^{VI}O_2/Mo^{V}O(OH)$ should be 7/2. In the absence of equilibrium 16, transfer of label to product $^{18}OPPh_3$ and loss via equilibrium 15 would lower the

(48) Craig, J. A.; Holm, R. H. *J. Am. Chem. Soc.* **1989**, *111*, 2111.
(49) Miller, K. F.; Wentworth, R. A. D. *Inorg. Chem.* **1979**, *18*, 984.
(50) Miller, K. F.; Wentworth, R. A. D. *Inorg. Chem.* **1980**, *19*, 1818.
(51) Corbin, J. L.; Miller, K. F.; Pariyadath, N.; Wherland, S.; Bruce, A. F.; Stiefel, E. I. *Inorg. Chim. Acta* **1984**, *90*, 41.
(52) Wilson, G. L.; Kony, M.; Tiekink, E. R. T.; Pilbrow, J. R.; Spence, J. T.; Wedd, A. G. *J. Am. Chem. Soc.* **1988**, *110*, 6923.
(53) Cannon, R. D. *Electron Transfer Reactions;* Butterworths: London, 1980.

total ^{18}O content of the Mo centers to a minimum of $85 \times (^7/_9) = 66$ atom %. After 7 h, the $LMoO_2(SPh)$ recovered after workup in air contained 55 atom % ^{18}O, supporting the existence of equilibrium 15. In addition, infrared spectra showed an excess of the $^{16}O^{18}O$ isotopomer, further evidence for equilibrium 16 (Figure 4).

The existence of equilibrium 15 allows direct incorporation of oxygen from H_2O into the Mo(V) center. In an attempt to provide direct evidence for the aquation of the $[Mo^{IV}O]^{2+}$ center (reaction 9), a reaction of $LMo^{16}O_2(SPh)$, PPh_3, and $H_2{}^{18}O$ (95 atom % ^{18}O) in THF was conducted under a positive pressure of $^{16}O_2$ with vigorous agitation. The proportion $Mo/PPh_3/H_2{}^{18}O = 1/3/20$ allowed an average of 3 turnovers per Mo center. After reaction was complete, the starting Mo complex $LMoO_2(SPh)$ was recovered in 90% yield and found to contain *ca.* 55 atom % ^{18}O. Inasmuch as little ^{18}O incorporation can be obtained through oxygen exchange at the Mo(VI) or Mo(V) levels due to the inertness of the former and the short life of the latter under the experimental conditions, this 55 atom % ^{18}O incorporation from $H_2{}^{18}O$ must be mainly achieved through water coordination at the Mo(IV) level (eq 9). The content of ^{18}O in $LMoO_2(SPh)$ is *ca.* 30% lower than that expected for 3 turnovers.[54] Possible reasons include dilution of the ^{18}O label by H_2O, H_2O_2, or HO_2 produced from reduction of $^{16}O_2$, coordination of H_2O_2 and HO_2 to the Mo(IV) center, and direct oxidation of PPh_3 by H_2O_2. Despite these complications, this work demonstrates that oxygen atoms transferred to PPh_3 from the $[Mo^{VI}O_2]^{2+}$ centers are primarily replaced by H_2O and not by O_2.

(54) Assuming a 95 atom % ^{18}O of H_2O in THF, each turnover should increase the ^{18}O label in $LMoO_2(SPh)$ by $0.5 \times 0.95 \times$ atom % ^{16}O in $LMoO_2(SPh)$. A content of 85 atom % ^{18}O in $LMoO_2(SPh)$ would be expected for 3 turnovers.

Conclusion

Reactions 2′−4′ of Scheme 3 have allowed development of a catalytic system which displays all the important centers and processes (reactions **2**−**4** of Scheme 1) proposed for catalysis by oxo−molybdenum enzymes featuring $[Mo^{VI}O_2]^{2+}$ active sites. Isotopic oxygen atom tracer studies demonstrate that the oxygen atom transferred to PPh_3 derives directly from the $[Mo^{VI}O_2]^{2+}$ centers and that water, not dioxygen, is the ultimate source of the oxygen atoms. The catalytic cycles feature OAT processes followed by CEPT processes to regenerate the active sites. The molybdenum center shuttles between three oxidation states—VI, IV, and V—during turnover. In the model system, catalytic activity is inhibited at the Mo(IV) level by a strongly coordinating solvent such as pyridine or poisoned by formation of either a stable Mo^V-OMe link or an oxo-bridged binuclear species. The formation of stable Mo^V-OR links appears to similarly terminate catalysis in certain $Mo^{VI}O_2$-based enzymes. Binucleation is not possible in such systems.

Acknowledgment. We thank Ms. M. A. Schwindt at the University of Melbourne for carrying out mass spectrometric measurements, and gratefully acknowledge financial support from the Australian Research Council (to C.G.Y. and A.G.W.) and the National Institutes of Health (Grant GM-37773 to J.H.E..).

Supporting Information Available: Text presenting X-ray experimental details and complete tables of crystallographic data, positional and thermal parameters, bond distances, bond angles, least-squares planes, dihedral angles, and torsional angles (11 pages). See any current masthead page for ordering information.

IC961065Z